;

# A DMSO-assisted iridium(III) complex as luminescent "turn-on"sensor for selective detection of L-histidine and bacterial imaging

Xiaojuan Li,[a] Tianqian Jia,[a] Yueyan Wang,[a] Yanyan Zhang,[a] Du Yang,[a] Sicheng Zhai[a] and Shuming Li*[b]

[a] School of Medical Engineering, Haojing College of Shaanxi University of Science & Technology, Xianyang 712046, Shaanxi, P.R. China.

[b] Co-construction Collaborative Innovation Center for Chinese Medicine Resources Industrialization by Shaanxi & Education Ministry, Shaanxi University of Chinese Medicine, Xianyang, 712083, Shaanxi, P.R. China. E-mail: 1501034@sntcm.edu.cn

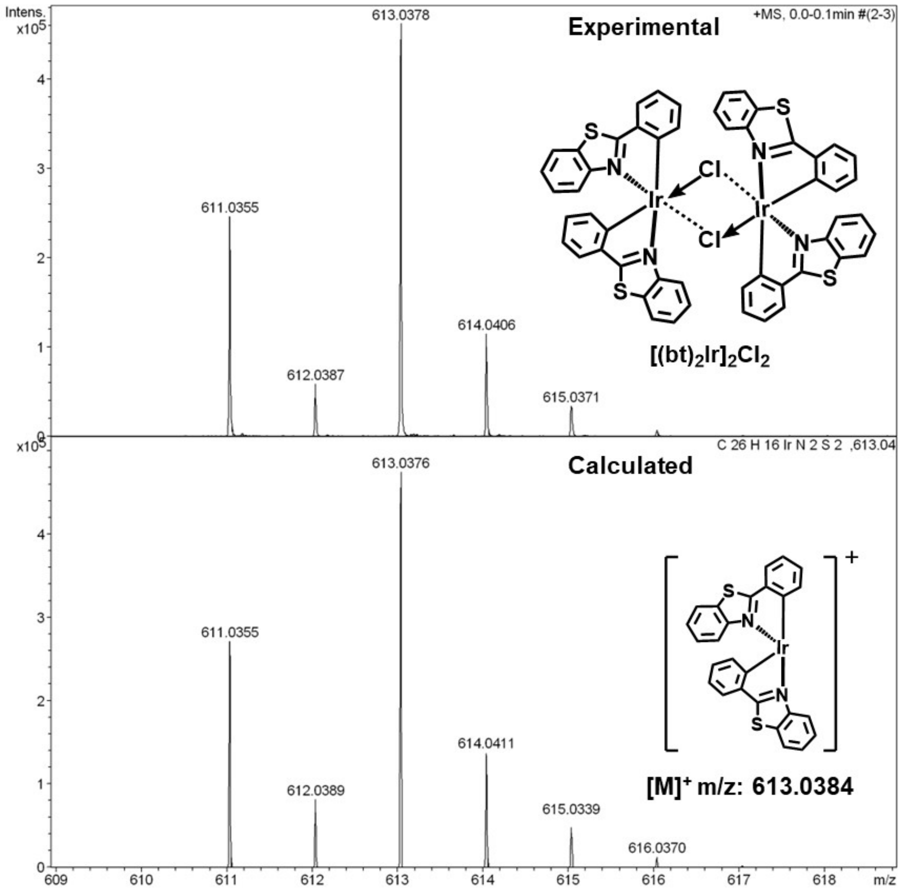


**Fig. S1** Mass spectrum of Ir1 experimental and calculated spectra of peak.

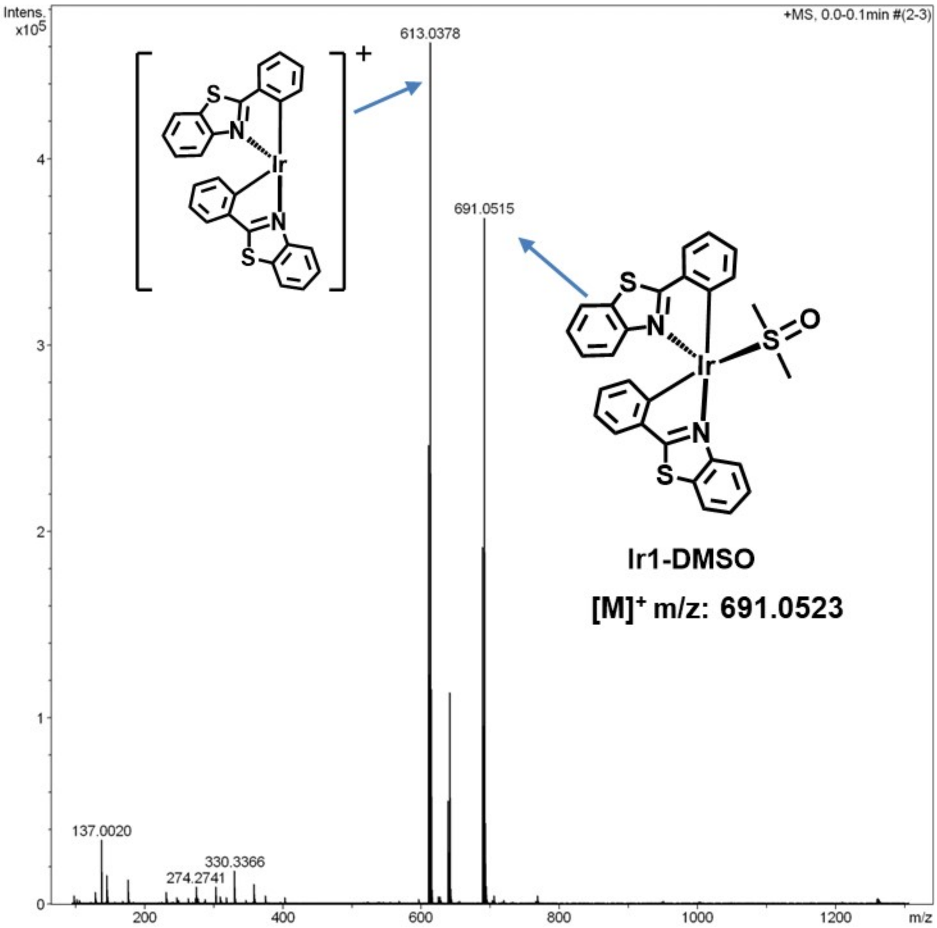


**Fig. S2** Mass spectrum of Ir1-DMSO experimental and calculated spectra of peak with m/z = 691.0523.

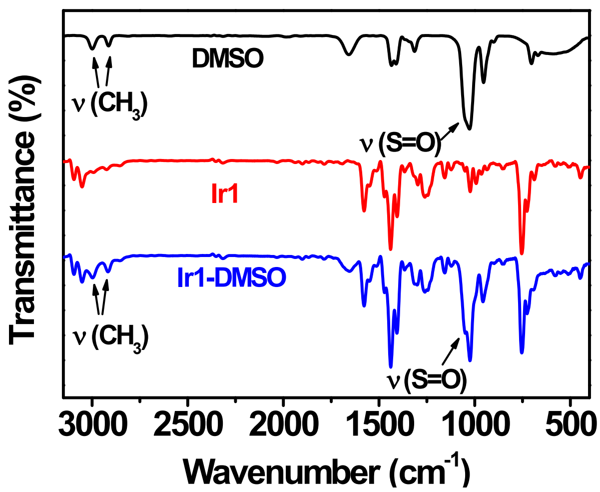


**Fig. S3** FTIR spectra of DMSO, Ir1, and Ir1-DMSO.

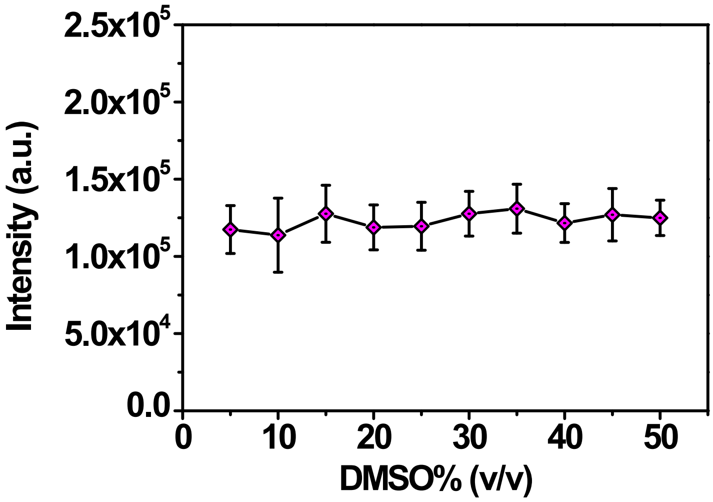


**Fig. S4** The PL intensity of Ir1in different volumes of DMSO solvent.

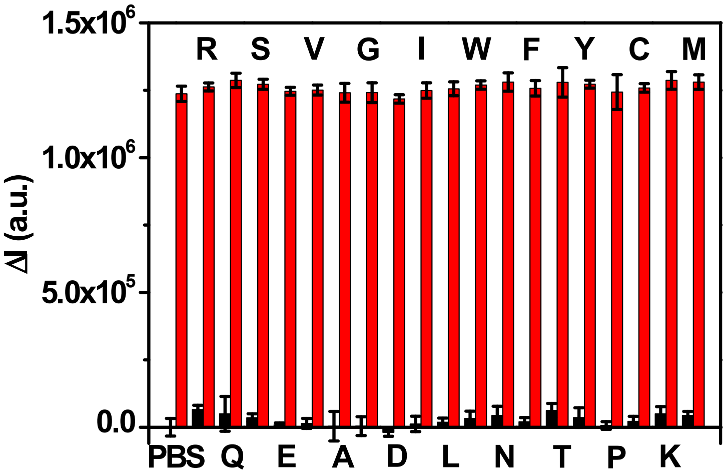


**Fig. S5** Relative emission intensity of Ir1-DMSO in presence and absence of L-His and others interfering amino acids (50 μM). $\Delta I = I - I_0$, I and $I_0$ represents the PL intensity of Ir1-DMSO with or without various amino acids.

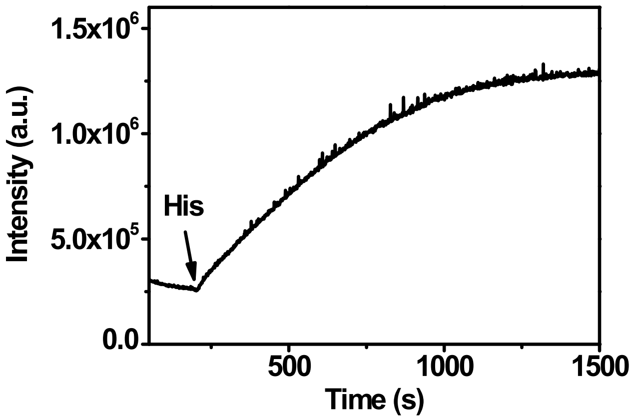


**Fig. S6** Time course of photoluminescence emission intensity of Ir1-DMSO before and after adding L-His.

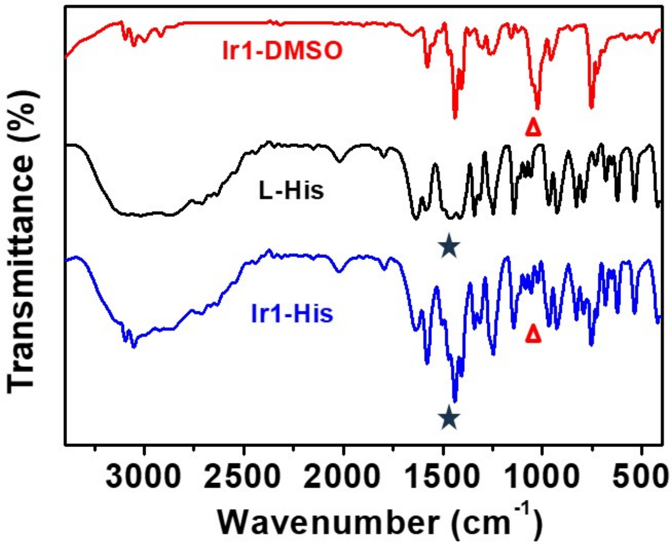


**Fig. S7** FTIR spectra of Ir1-DMSO, L-His, and Ir1-His.

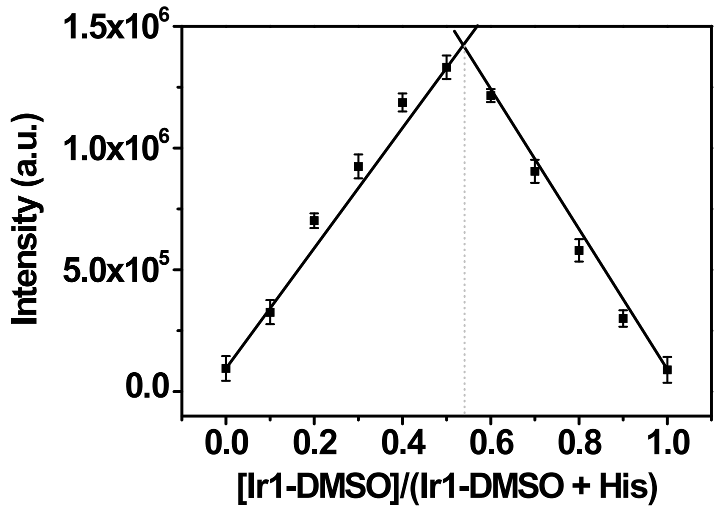


**Fig. S8** Job's plot of fluorescence intensity at 540 nm of Ir1-His *vs.* concentration fraction Ir1-DMSO for a total concentration (Ir1-DMSO + L-His) of 100 μM. The intersection of the two linear parts at 0.54.

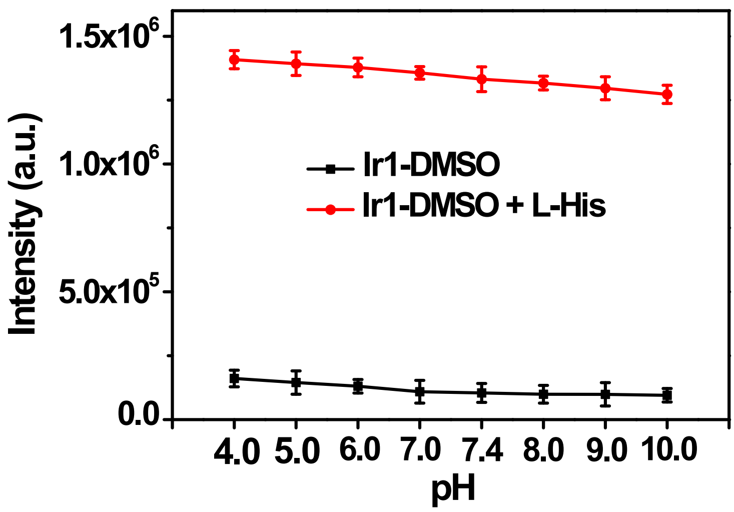


**Fig. S9** The PL intensity of Ir1-DMSO at 540 nm in the presence and absence of L-His in different pH solutions.

**Table S1** Comparison of linear range and detection limit for His assay

| Materials | Methods | Linear range | Detection limit | Ref. |
|---|---|---|---|---|
| o-Phthalaldehyde | Chromatography-Fluorescence | 0.5−25 μM | 160 nM | [S1] |
| lanthanide-based MOF ($Eu^{3+}$@Mn-MOF) | Fluorescence | 0−325 μM | 230 nM | [S2] |
| {$Zn_4$} cluster | Fluorescence | 5−32.5 μM | 830 nM | [S3] |
| Carbon Dots | Fluorescence | 0.05−10 μM | 35 nM | [S4] |
| Nitrogen-doped carbon nanoparticle | Fluorescence | 0.5−60 μM | 150 nM | [S5] |
| Bacterial Cellulose–Based MOF Hybrid | Fluorescence | 0.01–40 μM | 7 nM | [S6] |
| Iridium(III) complexes | Fluorescence | 2−32.5 μM | 35 nM | [S7] |
| Ir(III) solvent complex | Fluorescence | / | 620 nM | [S8] |
| Ir(III)-DMSO complex | Fluorescence | 0.2−10 μM | 80 nM | This work |

**Reference:**

[S1] E. Stampina, A. Tsiasioti, K. Klimatsaki, C. K. Zacharis and P. D. Tzanavaras, *J. Chromatogr. B* 2021, **1173**, 122697.

[S2] J. Xiao, L. Song, M. Liu, X. Wang and Z. Liu, *Inorg. Chem.* 2020, **59**, 6390–6397.

[S3] J. Li, K. Ma, Y. Yang, H. Yang, J. Lu, D. Li, J. Dou, H. Ma, S. Wang and Y. Li, *J. Mater. Chem. C*, 2022, **10**, 8979–8993.

[S4] W. Lu, Y. Jiao, Y. Gao, J. Qiao, M. Mozneb, S. Shuang, C. Dong and C. Li, *ACS Appl. Mater. Interfaces*, 2018, **10**, 42915−42924.

[S5] X. Zhu, T. Zhao, Z. Nie, Z. Miao, Y. Liu and S. Yao, *Nanoscale*, 2016, **8**, 2205−2211.

[S6] A. F. Kateshali, F. Moghzi, J. Soleimannejad and J. Janczak, *Inorg. Chem.,* 2024, **63**, 3560–3571.

[S7] L. Hu, X. Chen, K. Yu, N. Huang, H. Du, Y. Wei, Y. Wu and H. Wang, *Spectrochim. Acta A*, 2021, **262**, 120095.

[S8] H. Wang, B. Xu, H. Chen, D. Li, X. Shen, F. Cai, Y. Xu, L. Zhou and L. Hu, *Inorg. Chim. Acta*, 2020, **511**, 119799.